V International Conference on Computational Methods for Coupled Problems in Science and Engineering
COUPLED PROBLEMS 2013
S. Idelsohn, M. Papadrakakis and B. Schrefler (Eds)

COMPARISON BETWEEN TWO DIFFERENT DECOMPOSITIONS FOR THE SOLUTION OF FLUID-STRUCTURE INTERACTION PROBLEMS

JORIS DEGROOTE*, JORIS BOLS* AND LIESBETH TAELMAN†

*Department of Flow, Heat and Combustion Mechanics
Ghent University
Sint-Pietersnieuwstraat 41, B-9000 Ghent, Belgium
e-mail: Joris.Degroote@UGent.be, web page: http://www.FSI.UGent.be/

†IBiTech-bioMMeda
Ghent University
De Pintelaan 185, B-9000 Ghent, Belgium

Key words: Fluid-Structure Interaction, Gauss-Seidel iteration, Robin Boundary Condition, Artificial Compressibility

Abstract. Several types of decompositions and coupling algorithms can be used when solving a fluid-structure interaction problem in a partitioned way. In the case of Dirichlet-Neumann (DN) decomposition, the flow equations are solved with a Dirichlet boundary condition on the fluid-structure interface, while the structural equations are solved with a Neumann boundary condition on the interface. Robin-Neumann (RN) decomposition denotes a Robin boundary condition on the fluid side of the interface.

It is well-known that Gauss-Seidel iteration is often unstable for strongly coupled problems with DN decomposition. Conversely, this coupling algorithm can have good convergence properties in combination with RN decomposition. The Interface Artificial Compressibility (IAC) method is one of the techniques to improve the convergence of the Gauss-Seidel iterations for cases with DN decomposition.

In this paper, it is demonstrated that there is a common idea behind Gauss-Seidel iterations with RN decomposition and with DN decomposition plus IAC. Both approaches include a local, linear approximation for the structural equations into the flow equations. The numerical examples demonstrate that this approach is very suitable for the flow in flexible tubes, but that the application to other cases is not always straightforward.

1 INTRODUCTION

Different decompositions can be used for partitioned fluid-structure interaction simulations. They are characterized by the boundary conditions at the common boundary of the

fluid and the structure. In the case of Dirichlet-Neumann (DN) decomposition, the flow equations and the structural equations are solved with respectively a Dirichlet and a Neumann boundary condition on the fluid-structure interface. By contrast, Robin-Neumann (RN) decomposition implies a Robin boundary condition (i.e. a linear combination of a Dirichlet and a Neumann boundary condition) on the fluid side of the interface and a Neumann boundary condition on the structure side [1].

It is well-known that Gauss-Seidel (GS) or fixed-point iteration is often unstable for strongly coupled problems with DN decomposition [2]. Conversely, this coupling algorithm can have good convergence properties in combination with RN decomposition. To improve the convergence of the GS iterations for problems with DN decomposition, the Interface Artificial Compressibility (IAC) method has been proposed [3]. Despite the name, the IAC method uses a constant fluid density and the artificial source term disappears at convergence of the coupling iterations.

The remainder of this paper is organized as follows. Section 2 will explain that a local, linear approximation for the structural equations is included into the flow equations by both GS iterations with RN decomposition and with DN decomposition and IAC [4]. Subsequently, two numerical models are described in Section 3. Finally, the numerical examples in Section 4 will demonstrate that this approach is very suitable for the flow in flexible tubes, but that the application to other cases is not always straightforward.

2 COMPARISON

2.1 Interface conditions

On the fluid-structure interface Γ_i^{n+1}, the kinematic equilibrium condition

$$\vec{v}^{n+1} = \delta_t \vec{u}^{n+1} \tag{1a}$$

and the dynamic equilibrium condition

$$\bar{\sigma}_f^{n+1} \cdot \vec{n}^{n+1} = \bar{\sigma}_s^{n+1} \cdot \vec{n}^{n+1} \tag{1b}$$

need to be satisfied. $\vec{u}$ is the structural displacement, $\vec{v}$ the fluid velocity, $\vec{w}$ the grid velocity and $\bar{\sigma}_f$ the Cauchy stress tensor. The vector $\vec{n}$ is the normal pointing outwards of the fluid subdomain. Backward Euler time discretization is used for simplicity, so the notation δ_t refers to

$$\delta_t \vec{u}^{n+1} = \frac{\vec{u}^{n+1} - \vec{u}^n}{\Delta t}, \tag{1c}$$

with the superscript n denoting the time step and Δt the time step size.

In addition, the normal velocity of the fluid grid has to match the normal structural velocity on Γ_i^{n+1}.

$$\vec{w}^{n+1} \cdot \vec{n}^{n+1} = \delta_t \vec{u}^{n+1} \cdot \vec{n}^{n+1} \tag{1d}$$

Within each time step, GS coupling iterations are performed between the flow solver and the structural solver until some convergence criteria for the equilibrium conditions

on the fluid-structure interface are satisfied. The superscript $k+1$ indicates the current coupling iteration in the current time step $(n+1)$.

2.2 GS iterations with DN decomposition and IAC (GS-DN-IAC)

GS-DN uses a Dirichlet boundary condition on Γ_i^{k+1} for the flow equations, given by

$$\vec{v}^{k+1} = \delta_t \vec{u}^k \tag{2a}$$

For the grid velocity, a Dirichlet boundary condition

$$\vec{w}^k \cdot \vec{n}^k = \delta_t \vec{u}^k \cdot \vec{n}^k \tag{2b}$$

is applied. The values of $\vec{u}$ and $\vec{n}$ are determined by the structural calculation at the end of coupling iteration k.

While solving the structural equations, the most recent flow values are used in the Neumann boundary condition

$$\bar{\sigma}_s^{k+1} \cdot \vec{n}^{k+1} = \bar{\sigma}_f^{k+1} \cdot \vec{n}^{k+1}. \tag{2c}$$

When applying a finite volume discretization in arbitrary Lagrangian-Eulerian (ALE) formulation, the conservation of mass for an incompressible fluid is given by

$$\frac{V_i^k - V_i^n}{\Delta t} + \sum_j \left(\vec{v}_{i,j}^{k+1} - \vec{w}_{i,j}^k\right) \cdot \vec{n}_{i,j}^k S_{i,j}^k = 0, \tag{3}$$

with V_i the volume of cell i, $S_{i,j}$ the area of face j and $\vec{n}_{i,j}$ the normal pointing outwards. All geometrical values (including V_i, $S_{i,j}$ and $\vec{n}_{i,j}$) correspond with the structural calculation in the previous coupling iteration.

The IAC then adds the source term

$$-\frac{p_{i,m}^{k+1} - p_{i,m}^k}{\Delta t} \frac{\mathrm{d}\left(\vec{u}_{i,m} \cdot \vec{n}_{i,m}\right)}{\mathrm{d}p_{i,m}} S_{i,m}^k \tag{4}$$

to the right-hand side of Eq. (3) but only in cells adjacent to the fluid-structure interface. In [3], the coefficient $\mathrm{d}\left(\vec{u}_{i,m} \cdot \vec{n}_{i,m}\right)/\mathrm{d}p_{i,m}$ is calculated by finite differencing between two structural calculations for different pressures. Together with the first term of Eq. (3), the source term becomes a linear approximation for $(V_i^{k+1} - V_i^n)/\Delta t$.

Combination of the interface conditions for the fluid velocity (Eq. (2b)) and the grid velocity (Eq. (2a)) yields

$$\vec{w}^k \cdot \vec{n}^k = \delta_t \vec{u}^k \cdot \vec{n}^k = \vec{v}^{k+1} \cdot \vec{n}^k. \tag{5}$$

As a result, the second term in the continuity equation vanishes on the face $j = m$ that lies on the fluid-structure interface, giving

$$\frac{V_i^k - V_i^n}{\Delta t} + \sum_{j \neq m} \left(\vec{v}_{i,j}^{k+1} - \vec{w}_{i,j}^k\right) \cdot \vec{n}_{i,j}^k S_{i,j}^k = -\frac{p_{i,m}^{k+1} - p_{i,m}^k}{\Delta t} \frac{\mathrm{d}\left(\vec{u}_{i,m} \cdot \vec{n}_{i,m}\right)}{\mathrm{d}p_{i,m}} S_{i,m}^k \tag{6}$$

2.3 GS iterations with RN decomposition (GS-RN)

The GS-RN technique uses a Robin boundary condition on Γ_i^{k+1} for the fluid, given by

$$\vec{v}^{k+1} + \alpha\bar{\sigma}_f^{k+1} \cdot \vec{n}^k = \delta_t\vec{u}^k + \alpha\bar{\sigma}_s^k \cdot \vec{n}^k. \tag{7}$$

with α a coefficient. In [1], an analytical expression for this coefficient α is obtained by considering a membrane so that the structural equations can be written in the same form as the Robin boundary condition. Moreover, an optimal value for α derived from a Fourier analysis has been proposed in [5]. The boundary conditions for the grid velocity and for the structural equations are identical to those in Section 2.2.

By including the Robin condition, the factor $\left(\vec{v}_{i,j}^{k+1} - \vec{w}_{i,j}^k\right) \cdot \vec{n}_{i,j}^k$ for face $j = m$ on Γ_i^{k+1} becomes

$$\left(\vec{v}_{i,m}^{k+1} - \vec{w}_{i,m}^k\right) \cdot \vec{n}_{i,m}^k = \left(\delta_t\vec{u}_{i,m}^k + \alpha_{i,m}\left(\bar{\sigma}_{s,i,m}^k - \bar{\sigma}_{f,i,m}^{k+1}\right) \cdot \vec{n}_{i,m}^k - \vec{w}_{i,m}^k\right) \cdot \vec{n}_{i,m}^k. \tag{8a}$$

Substitution of Eq. (2b) and Eq. (2c) leads to

$$\left(\vec{v}_{i,m}^{k+1} - \vec{w}_{i,m}^k\right) \cdot \vec{n}_{i,m}^k = \alpha_{i,m}\vec{n}_{i,m}^k \cdot \left(\bar{\sigma}_{f,i,m}^k - \bar{\sigma}_{f,i,m}^{k+1}\right) \cdot \vec{n}_{i,m}^k. \tag{8b}$$

Subsequently, the summations in Eq. (3) are split into a term corresponding with face $j = m$ on Γ_i^{k+1} and the terms corresponding with the other faces $j \neq m$ not on Γ_i^{k+1}, giving

$$\frac{V_i^k - V_i^n}{\Delta t} + \sum_{j\neq m}\left(\vec{v}_{i,j}^{k+1} - \vec{w}_{i,j}^k\right) \cdot \vec{n}_{i,j}^k S_{i,j}^k = -\alpha_{i,m}\vec{n}_{i,m}^k \cdot \left(\bar{\sigma}_{f,i,m}^k - \bar{\sigma}_{f,i,m}^{k+1}\right) \cdot \vec{n}_{i,m}^k S_{i,m}^k \tag{9}$$

2.4 Equivalence

For many applications, $\bar{\sigma}_f$ can be simplified to $-p\bar{I}$. Consequently, Eq. (9) becomes

$$\frac{V_i^k - V_i^n}{\Delta t} + \sum_{j\neq m}\left(\vec{v}_{i,j}^{k+1} - \vec{w}_{i,j}^k\right) \cdot \vec{n}_{i,j}^k S_{i,j}^k = -\alpha_{i,m}\left(p_{i,m}^{k+1} - p_{i,m}^k\right) S_{i,m}^k \tag{10}$$

So, if the viscous tractions on the interface are small, Eq. (6) and Eq. (10) are equal if

$$\alpha_{i,m} = \frac{1}{\Delta t}\frac{\mathrm{d}\left(\vec{u}_{i,m} \cdot \vec{n}_{i,m}\right)}{\mathrm{d}p_{i,m}}. \tag{11}$$

The Navier-Stokes equations lead to the same result as this analysis based on the conservation of mass.

As could already be seen from Eq. (7), the coefficient $\alpha_{i,m}$ relates a change in velocity of the interface to a change in traction on the interface. If the parameter $\alpha_{i,m}$ (respectively $\mathrm{d}\left(\vec{u}_{i,m} \cdot \vec{n}_{i,m}\right)/\mathrm{d}p_{i,m}$) is set so that it approximates the actual velocity/traction (respectively displacement/pressure) relation of the structural model, then an approximation for the structural model is included into the flow calculation. This implies that both GS-RN and GS-DN-IAC take the fluid-structure interaction into account while solving the flow equations, as opposed to GS-DN.

3 MODELS

3.1 Tube

The first case is the propagation of a pressure wave in a two-dimensional axisymmetric flexible tube, as described in [6, 7]. This tube is a simplified model for a large artery. It has an inner radius of 0.005 m, a length of 0.05 m and a thickness of 0.001 m. The fluid is incompressible and has a density of 1000 kg/m^3 and a viscosity of 0.003 Pas. The tube's wall consists of a linear elastic material with density 1200 kg/m^3, Young's modulus 3×10^5 N/m^2 and Poisson's ratio 0.3. The structure is clamped in all directions at the inlet and outlet.

The finite volume flow solver Fluent 14.5 (Ansys Inc., Lebanon, NH, USA) uses second-order pressure interpolation, second-order upwind for the momentum and backward Euler for the time discretization. It solves the Navier-Stokes equations in arbitrary Lagrangian-Eulerian (ALE) formulation with the PISO scheme. The grid of the fluid domain is adapted to the displacement of the fluid-structure interface with a spring analogy. The finite element structural solver Abaqus 6.12 (Simulia Inc., Providence, RI, USA) uses implicit time integration of continuum elements with 8 nodes and reduced integration. The fluid grid consists of 100x10 cells, the structural grid of 50x5 elements.

Both the fluid and the structure are initially at rest. During the first 3×10^{-3} s, an overpressure of 1333.2 N/m^2 is applied at the inlet. The wave propagates through the tube during 10^{-2} s, simulated with time steps of 10^{-4} s.

3.2 Membrane pump

The second case is a two-dimensional axisymmetric model for a membrane pump [8]. This pump consists of a casing and a membrane with a hole at its middle to allow the fluid below the membrane to reach the outlet. The complete geometry is depicted in Figure 1. The radius and width of the casing are 46 mm and 11 mm, respectively. The membrane has an inner radius of 8 mm and, an outer radius of 38 mm and a thickness of 1 mm. The outer edge of the membrane is attached to an electromagnetic actuator which moves it up and down.

The fluid is water with a density of 998.2 kg/m^3 and a viscosity of 0.001003 kg/ms. The hyperelastic material of the structure is described with the Van der Waals model. It has a density of 1160 kg/m^3 and a stiffness between 1.4 and 2.3 N/mm^2.

The same flow solver and structural solver and the same discretization schemes as for the previous case have been applied. For this case with large deformation, cells in the fluid grid which are too large or too small are split or merged, respectively. The fluid grid initially consists of 8830 triangular cells, the structural grid of 40x4 elements.

Both the fluid and the structure are initially at rest. The actuator has an amplitude of 1 mm and a frequency of 50 Hz. The time step size is 0.5 ms.

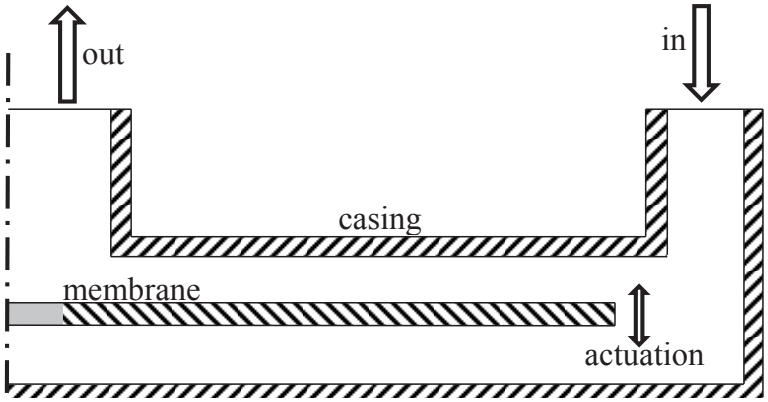

Figure 1: The geometry of the membrane pump.

Table 1: The average number of coupling iterations per time step for the propagation of the pressure wave in the flexible tube.

Algorithm	Iterations
GS-DN-IAC	4.0
IQN-ILS(5)	4.5
IQN-ILS(10)	3.6

4 RESULTS

The propagation of the pressure wave in the flexible tube has been calculated using the GS-DN-IAC algorithm [3] and the IQN-ILS algorithm [9]. Pressure contours at three instants are shown in Figure 2.

For each of these coupling algorithms, the number of coupling iterations in a time step is listed in Table 1, averaged over all time steps. The number between brackets behind IQN-ILS indicates from how many time steps data is reused by this algorithm. In each time step, the residual is reduced by three orders of magnitude with respect to its initial value in that time step. For this first case, the GS-DN-IAC algorithm performs similarly compared to the IQN-ILS algorithm. In addition to the 4 coupling iterations per time step, GS-DN-IAC requires two structural calculations to obtain the finite difference calculation of the compressibility factor.

Velocity vectors in the membrane pump are depicted in Figure 3. Despite various different attempts to calculate the compressibility coefficients for GS-DN-IAC, this scheme did not converge for this case. Using the IQN-ILS algorithm, on average 16 coupling iterations per time step are required if no data from previous time steps is reused.

For the flexible tube, the local structural model constructed by GS-DN-IAC and GS-RN is a good approximation of the structural behaviour. By contrast, the relation between

(a) 25 ms

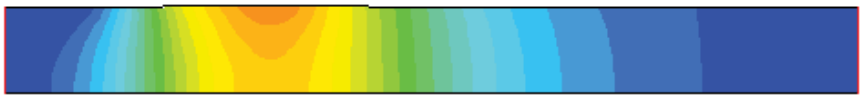

(b) 50 ms

(c) 75 ms

Figure 2: The pressure contours for the propagation of the pressure wave in the flexible tube.

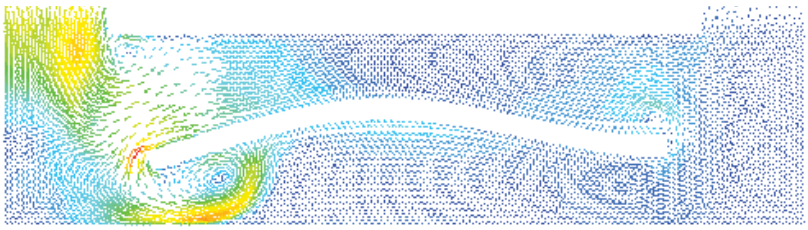

Figure 3: The velocity vectors in the membrane pump after 0.125 s.

the pressure and the displacement in the membrane pump will not be local. For example, the displacement of the membrane depends on the pressure difference between both sides of the membrane and not on the pressure on one side. As the structural response to a local change in pressure is not local, it can be expected that it can not be appoximated by a local model.

5 CONCLUSIONS

In this paper, it has been demonstrated that the Robin-Neumann decomposition and the Dirichlet-Neumann decomposition combined with Interface Artificial Compressibility both apply the same principle. They include a local, linear approximation for the structural behaviour into the flow solver. These techniques accelerate the convergence of Gauss-Seidel coupling iterations for the propagation of a pressure wave in a flexible tube. Yet, their application to a membrane pump is not straightforward.

REFERENCES

[1] S. Badia, F. Nobile, and C. Vergara. Fluid-structure partitioned procedures based on Robin transmission conditions. *J Comput Phys*, 227(14):7027–7051, 2008.

[2] P. Causin, J.-F. Gerbeau, and F. Nobile. Added-mass effect in the design of partitioned algorithms for fluid-structure problems. *Comput Meth Appl Mech Eng*, 194(42–44):4506–4527, 2005.

[3] J. Degroote, A. Swillens, P. Bruggeman, R. Haelterman, P. Segers, and J. Vierendeels. Simulation of fluid-structure interaction with the interface artificial compressibility method. *Comm Numer Meth Eng*, 26(3):276–289, 2010.

[4] J. Degroote. On the similarity between Dirichlet-Neumann with interface artificial compressibility and Robin-Neumann schemes for the solution of fluid-structure interaction problems. *J Comput Phys*, 230(17):6399–6403, 2011.

[5] L. Gerardo-Giorda, F. Nobile, and C. Vergara. Analysis and optimization of Robin-Robin partitioned procedures in fluid-structure interaction problems. *SIAM J Numer Anal*, 48(6):2091–2116, 2010.

[6] L. Formaggia, J.-F. Gerbeau, F. Nobile, and A. Quarteroni. On the coupling of 3D and 1D Navier-Stokes equations for flow problems in compliant vessels. *Comput Meth Appl Mech Eng*, 191(6–7):561–582, 2001.

[7] M.A. Fernandez and M. Moubachir. A Newton method using exact Jacobians for solving fluid-structure coupling. *Comput Struct*, 83(2–3):127–142, 2005.

[8] J. Bols, L. Taelman, J. Degroote, S. Annerel, and J. Vierendeels. Numerical analysis of the fluid-structure interaction in a membrane pump. In B.H.V. Topping, J.M.

Adan, F.J. Pallarés, R. Bru, and M.L. Romero, editors, *7th International Conference on Engineering Computational Technology*, pages 1–19, Valencia, Spain, September 2010.

[9] J. Degroote, K.-J. Bathe, and J. Vierendeels. Performance of a new partitioned procedure versus a monolithic procedure in fluid-structure interaction. *Comput Struct*, 87(11–12):793–801, 2009.